



Strengthening dust–cirrus relationships over Central Europe (2001–2025)

György Varga^{1,2}, Fruzsina Gresina¹, András Gelencsér^{2,3}, Adrienn Csávics¹, Ágnes Rostási^{2,3}

¹HUN-REN Research Centre for Astronomy and Earth Sciences, Budapest, Hungary

5 ²Research Institute of Biomolecular and Chemical Engineering, University of Pannonia, Veszprém, Hungary

³MTA-PE Air Chemistry Research Group, Research Institute of Biomolecular and Chemical Engineering, University of Pannonia, Veszprém, Hungary

Correspondence to: György Varga (varga.gyorgy@csfk.org)

Abstract. Saharan dust is increasingly recognized as an important driver of aerosol–cloud interactions over Europe, yet its
10 long-term influence on cloud formation remains poorly understood. This study investigates changes in the relationship between dust intrusions and upper-level cloud properties over the Carpathian Basin during the 2001–2025 period using a combination of MERRA-2 reanalysis, MODIS satellite observations, HIRS outgoing longwave radiation (OLR) data, and a database of 276 validated Saharan dust events.

The frequency of Saharan dust intrusions increased by nearly 70% during the study period. Dust outbreaks were associated
15 with enhanced high-cloud cover, increased cirrus reflectance, reduced effective ice particle radius, and lower OLR values. These relationships were particularly pronounced during spring, when thermodynamic conditions are most favourable for heterogeneous ice nucleation and cirrus development.

To quantify the temporal evolution of dust–cloud relationships, generalized additive models were applied to cloud and radiative
20 variables. Atmospheric dust loading was a highly significant predictor in all seasonal models, while significant dust–time interaction terms demonstrated that cloud responses to dust have systematically strengthened over time. The strongest signals were observed for cirrus reflectance, high-cloud fraction, and OLR, indicating increasingly pronounced upper-tropospheric cloud responses under comparable dust-loading conditions.

The results suggest that Saharan dust has become an increasingly important factor influencing cloud formation and radiative
25 processes over Central Europe. Together with growing evidence for more frequent ice-saturated and ice-supersaturated environments, the findings support the hypothesis that evolving upper-tropospheric conditions increasingly favour dust-associated cloud formation.

1. Introduction

Cirrus clouds represent one of the most important cloud types in the upper troposphere and play a key role in the Earth's
30 radiation budget and climate feedback processes (Lolli et al., 2026; Storelvmo, 2017; Twomey, 1974). Located at high altitudes and composed predominantly of ice crystals, cirrus clouds are capable of both partially reflecting incoming shortwave solar



radiation and absorbing and re-emitting outgoing longwave radiation from the Earth's surface (Boucher et al., 2013). Due to their low emission temperatures, cirrus clouds generally exert a positive radiative forcing, particularly when they are optically thin. Consequently, changes in cirrus cloud occurrence and upper-tropospheric humidity conditions have become a major focus of climate research.

35 In recent years, changes in upper-tropospheric cirrus conditions and ice-supersaturated regions (ISSRs) have attracted increasing scientific attention from a wide range of atmospheric observation and modelling studies (Benetatos et al., 2024; Sassen and Campbell, 2001). Observed changes in the Earth's radiation budget, the formation of extensive cirrus shields that can substantially reduce surface solar irradiance, and the climatic effects of persistent aircraft contrails and contrail-induced cirrus have all highlighted the importance of understanding upper-tropospheric cloud processes (Irvine and Shine, 2015; 40 Kärcher, 2018).

The geographical distribution of increasing ISSR occurrence exhibits considerable spatial variability. Particularly pronounced changes have been observed over the Northern Hemisphere mid-latitudes, including Europe and the North Atlantic region, where increases in ISSR frequency (+0.2 to +1.2% per decade) substantially exceed the global average. These short-lived yet microphysically critical atmospheric states provide favourable thermodynamic conditions for ice crystal formation. However, 45 the presence of suitable moisture conditions alone is insufficient for cirrus cloud development; effective ice-nucleating aerosol particles (Ice Nucleating Particles, INPs) are also required (Andreae and Rosenfeld, 2008; Kok et al., 2023; Storelvmo, 2017). In this context, Saharan mineral dust plays a particularly important role (Ansmann et al., 2019a; Seifert et al., 2023; Weger et al., 2018). During long-range transport events, large quantities of mineral dust can reach Europe, including Central Europe (Pey et al., 2013; Rogora et al., 2004; Salvador et al., 2022; Varga, 2020). Mineral aerosol particles, especially those rich in 50 quartz, calcite, and K-feldspar, are known to act as highly efficient heterogeneous ice nuclei under the low-temperature conditions of the upper troposphere (Chatziparaschos et al., 2023; Harrison et al., 2019; Hoose et al., 2008; Hoose and Möhler, 2012; Seifert et al., 2010). The presence of dust particles can promote ice crystal formation at lower supersaturation levels, increase ice crystal concentrations, and modify the optical thickness, reflectance, lifetime, and consequently the climatic effects of cirrus clouds (Benetatos et al., 2024; Kok et al., 2023; Storelvmo, 2017).

55 Increasing trends in both the frequency of Saharan dust intrusion events have been identified across Europe, including Central Europe, with the strongest increases occurring during approximately the last two decades (Cuevas-Agulló et al., 2024; Rodríguez and López-Darias, 2024; Salvador et al., 2022; Varga, 2020). According to regional dust climatologies, Saharan dust-laden air masses have reached Central Europe on average 8–12 times per year in recent years (Varga, 2020). The most pronounced reductions in solar irradiance have been observed during spring and autumn dust events, when indirect radiative effects 60 associated with cloud modification were found to play a dominant role (Varga et al., 2026). Previous studies have linked these changes to increasingly meridional atmospheric circulation patterns and a more meandering jet stream, which facilitate long-range dust transport while simultaneously influencing a wide range of hydrological and thermodynamic processes. Through



their impacts on multiple climate zones, these circulation changes may exert complex influences on cloud formation and persistence.

65 Despite these large-scale atmospheric changes, previous investigations have demonstrated that the contribution of Saharan dust to cirrus formation and the associated reduction in surface irradiance can be clearly identified and quantified. Enhanced cloud reflectance, increased optical thickness, and greater cloud persistence have been observed during dust intrusion events, indicating a substantial influence of mineral dust on cirrus cloud development (Varga et al., 2026). Nevertheless, long-term studies investigating regional trends in dust-associated cirrus changes remain scarce in Central Europe. In particular, there is
70 still limited understanding of the processes linking increasing Saharan dust activity, changing upper-tropospheric moisture conditions, and long-term modifications of cirrus cloud properties (Ansmann et al., 2019a; Seifert et al., 2023; Weger et al., 2018).

The present study aims to investigate long-term changes in cirrus clouds associated with Saharan mineral dust over the Carpathian Basin during the period 2001–2025. Particular emphasis is placed on assessing how increasingly frequent Saharan
75 dust intrusions influence the occurrence, reflectance, and seasonal behaviour of high-level ice clouds in Central Europe. The study focuses on the temporal evolution of aerosol–cloud interactions between mineral dust and cirrus clouds, especially during spring when conditions for heterogeneous ice nucleation are most favourable.

A further objective is to examine the extent to which the observed cirrus cloud changes may be linked to evolving upper-tropospheric moisture conditions and the increasing occurrence of ice-saturated and ice-supersaturated environments.

80 Although the study does not directly investigate ISSR climatology, the observed dust–cirrus relationships are interpreted within the broader context of ongoing thermodynamic changes in the upper troposphere.

2. Methods

2.1. Study area

The study focuses on the Carpathian Basin, with particular emphasis on Hungary and the surrounding Central European
85 regions. Due to its geographical location, the region is situated at the intersection of several major atmospheric circulation systems, where Atlantic, Mediterranean, and continental influences all play important roles. The basin-like topography favours the accumulation of air masses associated with long-range aerosol transport and provides favourable conditions for the formation and persistence of high-level cloud systems. The region is particularly sensitive to Saharan dust intrusions, which occur most frequently and intensely during the spring and summer seasons.



90 **2.2. Dust and cloud data**

Saharan dust events were investigated using data from the NASA Modern-Era Retrospective Analysis for Research and Applications Version 2 (MERRA-2) reanalysis. Atmospheric dust loading was characterized using hourly dust column mass density fields. Spatial and temporal variations in dust transport were analysed using country-scale and regional mean values. In addition to atmospheric dust loading, several satellite- and reanalysis-based datasets were employed to investigate the long-
95 term variability of cloud physical properties and radiative processes. Thermodynamic and cloud cover parameters of high-level clouds were obtained from the MERRA-2 reanalysis produced by NASA's Global Modeling and Assimilation Office. The cloud top pressure and cloud top temperature variables were used to characterize the vertical position and thermal properties of upper-level clouds, while the low, middle, and high cloud cover fraction datasets were used to assess seasonal and long-term variations in cloud cover at different atmospheric levels. MERRA-2 is a global atmospheric reanalysis based on
100 the Goddard Earth Observing System Model Version 5 (GEOS-5), incorporating both satellite and in situ observations through data assimilation.

To investigate the optical and microphysical properties of cirrus clouds, Level-3 products from the Moderate Resolution Imaging Spectroradiometer (MODIS) sensors onboard NASA's Terra and Aqua satellites were utilized. The cirrus reflectance dataset was used to characterize variations in the optical reflectivity of high-level ice clouds, while the ice cloud effective
105 particle radius variable provided estimates of the effective size of ice crystals within cirrus clouds. The Terra satellite has provided global observations since 1999, while Aqua has been operational since 2002, delivering continuous measurements of atmospheric and cloud properties.

Outgoing longwave radiation (OLR) was analysed using data from the High-resolution Infrared Radiation Sounder (HIRS) satellite instrument. OLR represents the amount of longwave radiation emitted from the Earth-atmosphere system to space
110 and is highly sensitive to the presence of high, cold cloud tops. Consequently, HIRS OLR observations provide a suitable basis for assessing the radiative impacts of dust-associated cirrus clouds and for examining their long-term variability over the study region.

2.3. Generalized additive model analysis

To quantify the relationships between atmospheric dust loading, cloud properties, and their temporal evolution, generalized
115 additive models (GAMs) were applied. GAMs represent a flexible extension of generalized linear models that allow the estimation of non-linear relationships through smooth functions fitted directly from the data. This approach is particularly suitable for atmospheric variables, where responses are often non-linear and may exhibit thresholds, saturation effects, or varying sensitivities across the investigated range.

For each investigated variable, separate seasonal models were constructed using daily dust column mass density thresholds
120 and the corresponding cloud and radiative parameters. The response variables included middle-, and high-level cloud fraction,



cirrus reflectance, effective ice particle radius, and outgoing longwave radiation. Atmospheric dust loading was introduced as a smooth predictor variable, while time was represented by the observation year.

The general model structure can be expressed as:

125
$$Y = \beta_0 + s(\text{Dust}) + s(\text{Time}) + \text{ti}(\text{Dust}, \text{Time}) + \varepsilon,$$

where Y denotes the investigated cloud or radiative variable, β_0 is the intercept, $s(\text{Dust})$ and $s(\text{Time})$ are smooth functions describing the non-linear effects of atmospheric dust loading and time, respectively, $\text{ti}(\text{Dust}, \text{Time})$ represents the tensor-product interaction between dust loading and time, and ε is the residual error term.

130 The smooth dust term was used to quantify the dependence of cloud and radiative properties on atmospheric dust loading, while the smooth time term was included to identify long-term changes during the 2001–2025 study period. The interaction term allowed the assessment of whether the sensitivity of the investigated variables to dust loading changed over time. Consequently, the GAM framework provided a means of evaluating not only the existence of dust–cloud relationships but also their temporal evolution.

135 Model performance was evaluated using adjusted coefficients of determination (adjusted R^2), while the statistical significance of individual smooth terms and interaction components was assessed using approximate F-tests and associated p-values. Statistical significance was assumed at $p < 0.05$. All GAM analyses were performed separately for each season in order to account for the strong seasonal variability of atmospheric dust transport and cloud formation processes over the Carpathian Basin. The GAMs were fitted using thin plate regression splines with smoothing parameters estimated by restricted maximum
140 likelihood.

2.4. Identification of Dust Events

Saharan dust intrusion events were identified using a multi-stage methodology consistent with previous studies, through which several hundred Saharan dust outbreaks have been documented between 1979 and the present (Varga, 2020; Varga et al., 2013). The existing database was further extended and updated within the framework of the present study. Potential dust events were
145 initially screened using daily aerosol index (AI) datasets derived from NASA’s Ozone Monitoring Instrument observations and MERRA-2 dust column mass density, which are well suited for detecting elevated concentrations of atmospheric mineral aerosols. The identified candidate events were subsequently validated using multiple independent data sources. Saharan origin was confirmed through the analysis of satellite imagery and backward air-mass trajectory calculations performed with the HYbrid Single-Particle Lagrangian Integrated Trajectory (HYSPLIT) model, which enabled the determination of source
150 regions and transport pathways (Stein et al., 2015).

The presence of mineral dust within the atmospheric column and its quantitative characterization were verified using the mapped (spatially represented) dust column mass density data from the MERRA-2 reanalysis. Monthly dry and wet dust deposition fields were additionally employed to assess dust loading and deposition processes. The synoptic meteorological

background of individual events was analysed using NCEP/NCAR reanalysis data, focusing primarily on the 700-hPa and
155 500-hPa geopotential height fields and the associated zonal and meridional wind components (for a detailed methodological
description see (Varga, 2020)).

Beyond the analysis of discrete dust events, the relationship between atmospheric dust loading and cloud-formation processes
was investigated using continuous dust column mass density thresholds. Days were classified according to the observed
atmospheric dust load. Because no universally accepted threshold exists for distinguishing dusty and non-dusty conditions
160 across different geographical and climatic environments, and seasons, multiple dust-loading thresholds were applied. Dust
column mass density threshold values were systematically varied between 0 and 0.006 g m⁻² in increments of 0.0001 g m⁻².
For each threshold value, daily mean cloud parameters, including cirrus reflectance, high cloud cover fraction, and effective
ice particle radius, were calculated and subsequently analysed seasonally within consecutive five-year time windows across
the 2001–2025 study period.

165 This approach enabled the assessment of how different dust-loading regimes are associated with changes in the optical and
spatial characteristics of cirrus clouds. To evaluate radiative impacts, the same methodology was applied to ice cloud effective
particle radius, cloud fractions (at different heights), outgoing longwave radiation (OLR) data, allowing the investigation of
long-term relationships between atmospheric dust loading, cirrus cloud development, and upper-tropospheric radiative
processes.

170 3. Results

3.1. Frequency and synoptic types of Saharan dust events

A total of 276 Saharan dust events (SDEs) were identified over the Carpathian Basin during the 2001–2025 study period (Table
1, Figure 1). The seasonal distribution of events was strongly asymmetric, with spring accounting for the highest number of
dust intrusions (116 events), representing approximately 42% of all identified cases. The spring maximum was followed by
175 summer with 72 events, while 46 and 42 events were recorded during autumn and winter, respectively. Mean dust loading was
also highest during spring, reaching 0.008 g m⁻², whereas average dust column mass density values ranged between 0.005 and
0.006 g m⁻² in the remaining seasons.

Analysis of consecutive five-year periods revealed a clear increasing trend in the frequency of dust events. While 40 events
were identified during 2001–2005, the number increased to 48 during 2006–2010, 60 during 2011–2015, 61 during 2016–
180 2020, and 67 during 2021–2025. This corresponds to an increase of nearly 70% relative to the beginning of the study period.
The increase was primarily driven by a growing number of spring and summer dust outbreaks. Spring events increased from
18 to 29 cases, while summer events rose from 11 to 19. Autumn also exhibited a moderate increase, from 8 to 14 events,
whereas winter dust intrusions showed no clear long-term trend.

In contrast, the intensity of dust loading did not display a similarly pronounced increase. Average dust column mass density
185 values remained within a relatively narrow range of 0.005–0.009 g m⁻² throughout the different five-year periods. These results



suggest that the observed long-term changes are primarily associated with an increasing frequency of Saharan dust intrusions rather than a systematic intensification of individual events. The strongest seasonal signal remained evident during spring, which exhibited both the highest event frequency and the greatest average dust loading, highlighting the dominant role of the spring season in Central European dust transport and related atmospheric processes.

190 The classification of events according to their synoptic background revealed substantial differences in dust transport characteristics and associated cloud properties. Type 1 events are characterized by a pronounced pressure gradient between a deep trough over the eastern North Atlantic and a high-pressure system extending across the Mediterranean and North Africa. In many cases, cut-off lows detached from the parent trough trigger intense dust storms within the intramontane basins of the Atlas Mountains, and in the forefront of the mountain range. The resulting dust plumes are subsequently transported toward
195 Central Europe by southwesterly flow.

Type 2 events are associated with Mediterranean cyclones, during which dust is advected into the study region within the warm sector and ahead of the cyclone. Type 3 events are characterized by the longest transport pathways. In these cases, an anticyclonic circulation over the northwestern Sahara transports dust from western Saharan source regions toward the eastern and northeastern Atlantic, from where prevailing westerlies subsequently carry the aerosol plume toward Central Europe.

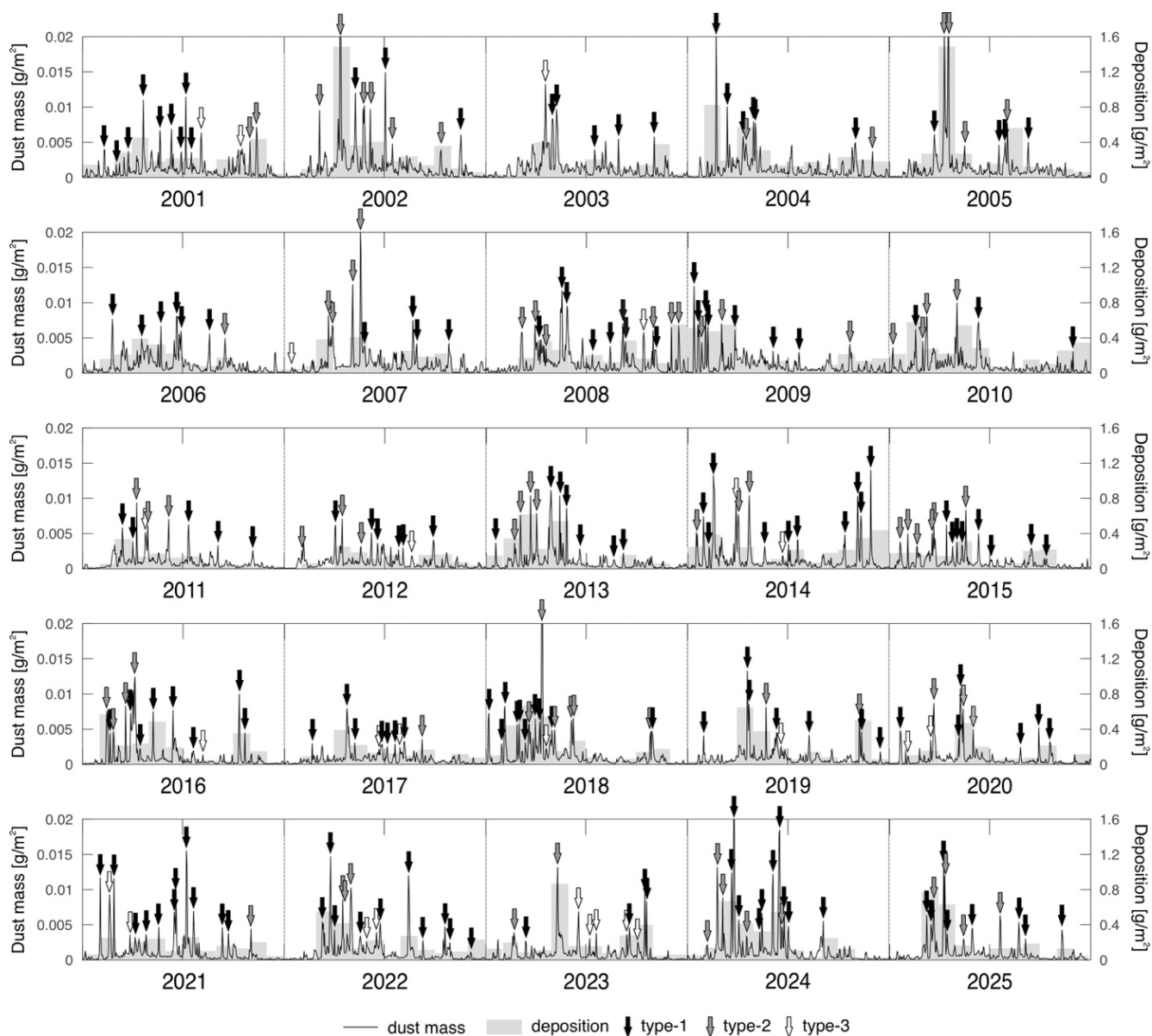
200 Considering the entire study period, Type 1 represented the most frequent synoptic category with 101 identified events. Type 2 accounted for 53 events, whereas only 9 cases were classified as Type 3. The highest average dust loading was observed for Type 2 events (0.011 g m^{-2}), while Type 1 and Type 3 episodes exhibited similar mean dust column mass density values of approximately $0.007\text{--}0.008 \text{ g m}^{-2}$.

205 **Table 1. Seasonal and total frequency and intensity of Saharan dust events (SDEs) over the Carpathian Basin during the 2001–2025 period.**

| Timeframe | Winter | | Spring | | Summer | | Autumn | | Total | |
|------------------|----------|-------------------------------------|-----------|-------------------------------------|-----------|-------------------------------------|----------|-------------------------------------|-----------|-------------------------------------|
| | SDEs (n) | Dust mass (avg.) [g/m^2] | SDEs (n) | Dust mass (avg.) [g/m^2] | SDEs (n) | Dust mass (avg.) [g/m^2] | SDEs (n) | Dust mass (avg.) [g/m^2] | SDEs (n) | Dust mass (avg.) [g/m^2] |
| 2001-2005 | 3 | 0.009 | 18 | 0.011 | 11 | 0.007 | 8 | 0.005 | 40 | 0.009 |
| 2001 | 1 | 0.004 | 4 | 0.006 | 3 | 0.008 | 3 | 0.005 | 11 | 0.006 |
| 2002 | | | 4 | 0.015 | 3 | 0.010 | 2 | 0.005 | 9 | 0.011 |
| 2003 | | | 3 | 0.010 | 2 | 0.005 | 1 | 0.006 | 6 | 0.008 |
| 2004 | 2 | 0.012 | 3 | 0.009 | | | 1 | 0.005 | 6 | 0.009 |
| 2005 | | | 4 | 0.013 | 3 | 0.006 | 1 | 0.005 | 8 | 0.009 |



| | | | | | | | | | | |
|------------------|-----------|--------------|------------|--------------|-----------|--------------|-----------|--------------|------------|--------------|
| 2006-2010 | 12 | 0.006 | 18 | 0.007 | 10 | 0.005 | 8 | 0.005 | 48 | 0.006 |
| 2006 | 1 | 0.008 | 2 | 0.005 | 3 | 0.007 | 1 | 0.005 | 7 | 0.006 |
| 2007 | 1 | 0.001 | 5 | 0.010 | 2 | 0.006 | 1 | 0.004 | 9 | 0.008 |
| 2008 | 2 | 0.007 | 6 | 0.006 | 2 | 0.003 | 5 | 0.005 | 15 | 0.006 |
| 2009 | 5 | 0.008 | 2 | 0.007 | 2 | 0.003 | 1 | 0.004 | 10 | 0.006 |
| 2010 | 3 | 0.004 | 3 | 0.008 | 1 | 0.007 | | | 7 | 0.006 |
| 2011-2015 | 12 | 0.006 | 25 | 0.007 | 16 | 0.003 | 7 | 0.004 | 60 | 0.005 |
| 2011 | 1 | 0.000 | 5 | 0.006 | 2 | 0.007 | 2 | 0.003 | 10 | 0.005 |
| 2012 | 1 | 0.004 | 3 | 0.005 | 5 | 0.003 | 1 | 0.004 | 10 | 0.004 |
| 2013 | 2 | 0.004 | 6 | 0.009 | 3 | 0.002 | | | 11 | 0.006 |
| 2014 | 5 | 0.009 | 4 | 0.007 | 4 | 0.003 | 2 | 0.008 | 15 | 0.007 |
| 2015 | 3 | 0.004 | 7 | 0.005 | 2 | 0.003 | 2 | 0.002 | 14 | 0.004 |
| 2016-2020 | 10 | 0.004 | 26 | 0.008 | 16 | 0.003 | 9 | 0.005 | 61 | 0.006 |
| 2016 | 2 | 0.006 | 6 | 0.007 | 3 | 0.003 | 2 | 0.007 | 13 | 0.006 |
| 2017 | 1 | 0.003 | 2 | 0.005 | 6 | 0.002 | 1 | 0.004 | 10 | 0.003 |
| 2018 | 3 | 0.006 | 10 | 0.008 | 2 | 0.006 | 2 | 0.005 | 17 | 0.007 |
| 2019 | 2 | 0.003 | 3 | 0.010 | 3 | 0.003 | 2 | 0.006 | 10 | 0.006 |
| 2020 | 2 | 0.003 | 5 | 0.007 | 2 | 0.004 | 2 | 0.004 | 11 | 0.005 |
| 2021-2025 | 5 | 0.006 | 29 | 0.008 | 19 | 0.007 | 14 | 0.005 | 67 | 0.007 |
| 2021 | 2 | 0.010 | 5 | 0.005 | 4 | 0.010 | 3 | 0.004 | 14 | 0.007 |
| 2022 | 1 | 0.001 | 7 | 0.007 | 4 | 0.006 | 3 | 0.003 | 15 | 0.006 |
| 2023 | 1 | 0.004 | 2 | 0.008 | 3 | 0.005 | 5 | 0.006 | 11 | 0.006 |
| 2024 | 1 | 0.002 | 8 | 0.010 | 5 | 0.009 | 1 | 0.005 | 15 | 0.009 |
| 2025 | | | 7 | 0.007 | 3 | 0.005 | 2 | 0.004 | 12 | 0.006 |
| Total | 42 | 0.006 | 116 | 0.008 | 72 | 0.005 | 46 | 0.005 | 276 | 0.006 |



210 **Figure 1. Temporal evolution of atmospheric dust loading, dust deposition, and the frequency and synoptic classification of Saharan dust events over the Carpathian Basin during the 2001–2025 period. (Type-1, type-2, and type-3 refer to the synoptic types of dust storm events described in the text.)**

3.2. Relationship between atmospheric dust and cloud formation processes

The characteristics of high-level cloud cover revealed clear differences among the three synoptic categories. The highest mean
 215 high cloud fraction was observed for Type 2 events (0.62), while somewhat lower values were associated with Type 1 situations (0.52), and substantially lower high-cloud coverage characterized Type 3 events (0.31). Similar differences were found for



cirrus reflectance. The mean reflectance of Type 2 events (0.22) was approximately twice that observed for Type 1 events (0.10), whereas Type 3 situations exhibited extremely low reflectance values (0.017). These findings indicate that Type 2 synoptic conditions are the most favourable for the development of extensive and optically mature cirrus cloud systems.

220 The effective radius of ice crystals also exhibited substantial differences among the synoptic categories. The smallest mean particle sizes were associated with Type 2 events (29.5 μm), while larger effective radii occurred during Type 1 and especially Type 3 situations. The simultaneous occurrence of smaller ice crystal sizes and higher cirrus reflectance in the Type 2 category may indicate more intense heterogeneous ice nucleation processes and higher ice particle number concentrations.

The importance of synoptic conditions also changed over time. The frequency of Type 1 situations increased throughout the study period, particularly during 2011–2015, while Type 2 events remained frequent during the most recent years. Concurrently, both dominant synoptic categories exhibited increasing high cloud cover fractions and cirrus reflectance values, suggesting that similar large-scale meteorological conditions have become increasingly associated with enhanced upper-level ice cloud formation in recent decades. Owing to its low occurrence frequency and comparatively weak cloud-related characteristics, Type 3 appears to be of secondary importance in terms of dust–cirrus interactions.

225

230 Using the complete database of 276 Saharan dust events, cirrus conditions were characterized based on the distributions of cirrus reflectance and high cloud fraction. The moderately affected category included events for which both cirrus reflectance and high cloud fraction fell between the second and third quartiles (cirrus reflectance: 0.089–0.178; high cloud fraction: 0.599–0.779). The strongly affected category consisted of events for which both parameters exceeded the third quartile, while all remaining cases were classified as other events.

235 According to this classification, 35 events (12.7%) belonged to the strongly affected category, 24 events (8.7%) were classified as moderately affected, and 217 events (78.6%) fell into the other category. Dust loading increased systematically with the degree of cirrus involvement. Mean dust mass values increased from 0.0059 g m^{-2} in the other category to 0.0068 g m^{-2} in the moderately affected group and reached 0.0091 g m^{-2} in the strongly affected category. This represents an increase of nearly 55% between the weakest and strongest cirrus-related categories.

240 At the same time, the effective radius of ice crystals exhibited a decreasing tendency. Mean particle size declined from 30.3 μm in the other-event category to 29.9 μm in the moderately affected group and further decreased to 28.2 μm in the strongly affected category. The combination of higher dust loading, smaller ice crystal sizes, and enhanced cirrus reflectance is consistent with the hypothesis that Saharan mineral dust acts as an efficient heterogeneous ice-nucleating particle, promoting the formation of cirrus clouds characterized by higher ice particle number concentrations.

245 The seasonal distribution also showed pronounced differences. Nearly half of the strongly affected events occurred during spring (17 cases), while a substantial number were also recorded during winter (12 cases). Autumn and summer occurrences were considerably less frequent (4 and 2 events, respectively). A similar seasonal pattern emerged for the moderately affected category, where spring events dominated (10 cases), followed by summer (7 cases) and winter (5 cases). Overall, the results indicate that the most intense cirrus-forming situations are primarily associated with springtime dust intrusions and are

250 systematically characterized by higher dust loading and smaller effective ice crystal sizes.



To investigate long-term changes in dust–cirrus relationships, Saharan dust events were grouped according to cirrus reflectance and high cloud fraction. When the two parameters were combined to identify the most strongly cirrus-affected events, no clear increasing trend emerged, and the maximum number of such cases occurred during the 2011–2015 period. However, the relatively low number of events limits the robustness of long-term trend assessments.

255 When the two parameters were analysed separately, considerably stronger trends became apparent. The number of events characterized by cirrus reflectance values above the upper quartile increased from 11 during 2001–2005 to 19 during 2021–2025, indicating that optically developed cirrus clouds have become increasingly common. These events were generally associated with smaller effective ice crystal radii, consistent with enhanced heterogeneous ice nucleation.

An even stronger change was observed for high cloud fraction. The number of events exceeding the upper quartile threshold 260 increased from approximately 6–8 events per five-year period at the beginning of the study interval to 19–20 events after 2016. This more than threefold increase suggests that an increasing proportion of Saharan dust intrusions are associated with extensive upper-level cloud cover.

Overall, the strongest and most robust long-term signal is not necessarily reflected in an increasing number of extremely intense cirrus events, but rather in the growing proportion of dust outbreaks that are accompanied by optically developed and 265 particularly extensive upper-tropospheric ice cloud systems.

Table 2. Changes in the frequency of cirrus-associated Saharan dust events (SDEs) according to different classification approaches during the 2001–2025 period.

| Classification | 2001– 2005 | 2006– 2010 | 2011– 2015 | 2016– 2020 | 2021– 2025 | Change (%) |
|---|---------------|---------------|---------------|---------------|---------------|---------------|
| Cirrus reflectance > Q3* (episodes) | 11 | 10 | 16 | 13 | 19 | 73 |
| High cloud fraction > Q3 (episodes) | 8 | 6 | 16 | 20 | 19 | 138 |
| Cirrus reflectance > Q3 AND High cloud fraction > Q3 (episodes) | 3 | 4 | 12 | 9 | 7 | 133** |
| All SDEs | 40 | 48 | 60 | 61 | 67 | 67 |

*Q3 refers to 3rd (upper) quartile of the given parameter

270 **Due to the low number of events in the baseline period, the relative change should be interpreted with caution.

3.3. Generalized additive model analysis of dust–cloud relationships

To quantify the relationships between atmospheric dust loading, five cloud and radiation properties, and their temporal evolution, generalized additive models (GAMs) were applied separately for each season and investigated variable (4×5 models). The models included smooth functions of dust column mass density and time, as well as their interaction term, 275 allowing the assessment of both non-linear dust responses and temporal changes in dust sensitivity.



The GAM analysis revealed highly significant relationships between atmospheric dust loading and all investigated cloud and radiative variables (Table 3.). The smooth dust term was statistically significant in all 20 seasonal models ($p < 0.001$), indicating that dust loading explains a substantial fraction of the observed variability in cloud and radiation characteristics. Model performance was generally high, with adjusted R^2 values ranging between approximately 0.89 and 0.996, demonstrating a strong ability of the models to reproduce the observed patterns.

The strongest dust dependence was identified for cirrus reflectance, high cloud fraction, and OLR, particularly during spring. In these cases, the fitted smooth functions revealed pronounced non-linear responses across the investigated dust-loading range. Effective ice particle radius also exhibited a significant dust-related response in all seasons, whereas middle-, and high-level cloud fractions showed systematic variations with increasing dust concentration.

The temporal component of the GAM models was likewise significant in the majority of cases. Twelve of the twenty seasonal models exhibited statistically significant smooth time terms, indicating that several cloud and radiative parameters experienced measurable long-term changes during the 2001–2025 study period. The most pronounced temporal signals were observed for spring cirrus reflectance, effective ice particle radius, middle- and high-level cloud fraction, and OLR.

A particularly robust result emerged from the interaction between atmospheric dust loading and time. The dust–time interaction term was statistically significant in all investigated models, demonstrating that the relationship between dust loading and cloud properties was not constant throughout the study period. This finding indicates that the response of cloud and radiative variables to increasing dust concentrations changed systematically between 2001 and 2025.

Among all investigated variables, cirrus reflectance exhibited the strongest overall model performance, with adjusted R^2 values approaching 1.00 in several seasons. High cloud fraction and OLR produced similarly strong fits, whereas effective ice particle radius and middle cloud fraction also showed consistently high explanatory power. Collectively, the GAM analysis demonstrates that atmospheric dust loading represents a statistically significant predictor of cloud optical, microphysical, and radiative properties throughout the study period and that these relationships exhibit substantial temporal variability.

Table 3. Generalized additive model (GAM) statistics describing the relationships between atmospheric dust loading and cloud and radiative variables during 2001–2025. (Adj. R^2 is the adjusted coefficient of determination. $p(\text{Dust})$, $p(\text{Time})$, and $p(\text{Dust} \times \text{Time})$ denote the significance of the dust effect, temporal trend, and their interaction, respectively. A significant dust \times time interaction indicates changing dust sensitivity over the study period.)

| Variable | Season | Adj. R^2 | $p(\text{Dust})$ | $p(\text{Time})$ | $p(\text{Dust} \times \text{Time})$ | Change in dust effect* | Strengthening |
|--------------------|--------|------------|------------------------|------------------|-------------------------------------|------------------------|---------------|
| Cirrus reflectance | Winter | 0.973 | 1.5×10^{-167} | 0.072 | 1.0×10^{-144} | −0.149 | No |
| | Spring | 0.996 | 1.5×10^{-136} | 0.002 | 1.1×10^{-193} | 0.095 | Yes |
| | Summer | 0.939 | 2.9×10^{-107} | 0.141 | 1.2×10^{-69} | −0.038 | No |
| | Autumn | 0.957 | 4.9×10^{-110} | 0.589 | 1.3×10^{-110} | −0.074 | No |



| | | | | | | | |
|-----------------------------|--------|-------|------------------------|-----------------------|------------------------|--------|-----|
| Particle radius | Winter | 0.893 | 4.7×10^{-43} | 2.5×10^{-5} | 8.2×10^{-58} | -0.509 | Yes |
| | Spring | 0.979 | 1.3×10^{-56} | 2.2×10^{-25} | 1.5×10^{-93} | -1.492 | Yes |
| | Summer | 0.98 | 8.8×10^{-35} | 1.1×10^{-10} | 1.6×10^{-166} | 0.797 | Yes |
| | Autumn | 0.895 | 1.9×10^{-56} | 0.017 | 8.5×10^{-90} | -3.352 | Yes |
| Mid cloud fraction | Winter | 0.966 | 5.9×10^{-103} | 0.003 | 5.7×10^{-122} | -0.116 | No |
| | Spring | 0.981 | 5.4×10^{-114} | 1.0×10^{-6} | 2.7×10^{-116} | 0.075 | Yes |
| | Summer | 0.921 | 3.0×10^{-56} | 0.017 | 7.2×10^{-107} | -0.012 | No |
| | Autumn | 0.97 | 9.9×10^{-69} | 9.6×10^{-5} | 2.5×10^{-145} | 0.077 | Yes |
| High cloud fraction | Winter | 0.986 | 7.1×10^{-159} | 0.006 | 1.9×10^{-180} | -0.497 | No |
| | Spring | 0.993 | 7.2×10^{-151} | 4.2×10^{-11} | 8.0×10^{-130} | 0.155 | Yes |
| | Summer | 0.952 | 2.3×10^{-40} | 0.214 | 2.0×10^{-90} | 0.042 | Yes |
| | Autumn | 0.985 | 1.6×10^{-69} | 0.049 | 9.1×10^{-144} | 0.264 | Yes |
| Outgoing longwave radiation | Winter | 0.968 | 2.4×10^{-152} | 0.005 | 4.5×10^{-158} | -8.64 | No |
| | Spring | 0.988 | 1.8×10^{-138} | 5.0×10^{-6} | 7.0×10^{-95} | -7.23 | Yes |
| | Summer | 0.94 | 4.6×10^{-66} | 0.083 | 2.2×10^{-85} | -4.56 | No |
| | Autumn | 0.968 | 1.8×10^{-92} | 0.052 | 2.2×10^{-124} | -29.52 | Yes |

*Change in dust effect represents the difference between the modelled dust response during the final (2021–2025) and initial (2001–2005) periods. Positive values indicate strengthening positive dust responses, whereas negative values indicate increasingly negative responses. All dust smooth terms and dust \times time interaction terms were statistically significant ($p < 0.001$).

3.4. Dust and cirrus clouds in spring

Based on the above results, the analysis was restricted to the spring season, as the investigated dust–cirrus interactions were most pronounced and consistent during this period. Although autumn also represents a transitional season and, in several respects, provides favourable conditions for upper-tropospheric moistening and high-level cloud formation, the observed relationships were considerably weaker and less coherent. During summer, the warm to hot atmospheric conditions that frequently develop over Central Europe are generally less favourable for cirrus formation, as upper-tropospheric temperature and moisture conditions often do not satisfy the thermodynamic requirements necessary for the development of ice-saturated or ice-supersaturated environments. Furthermore, enhanced convective activity and lower relative atmospheric water vapor values during summer can substantially modify the relationship between high-level cloud cover and longwave radiative processes. In winter, by contrast, Saharan dust intrusions occur much less frequently, while cloud formation is primarily controlled by large-scale cyclonic and frontal processes. Consequently, spring provides particularly favourable conditions for



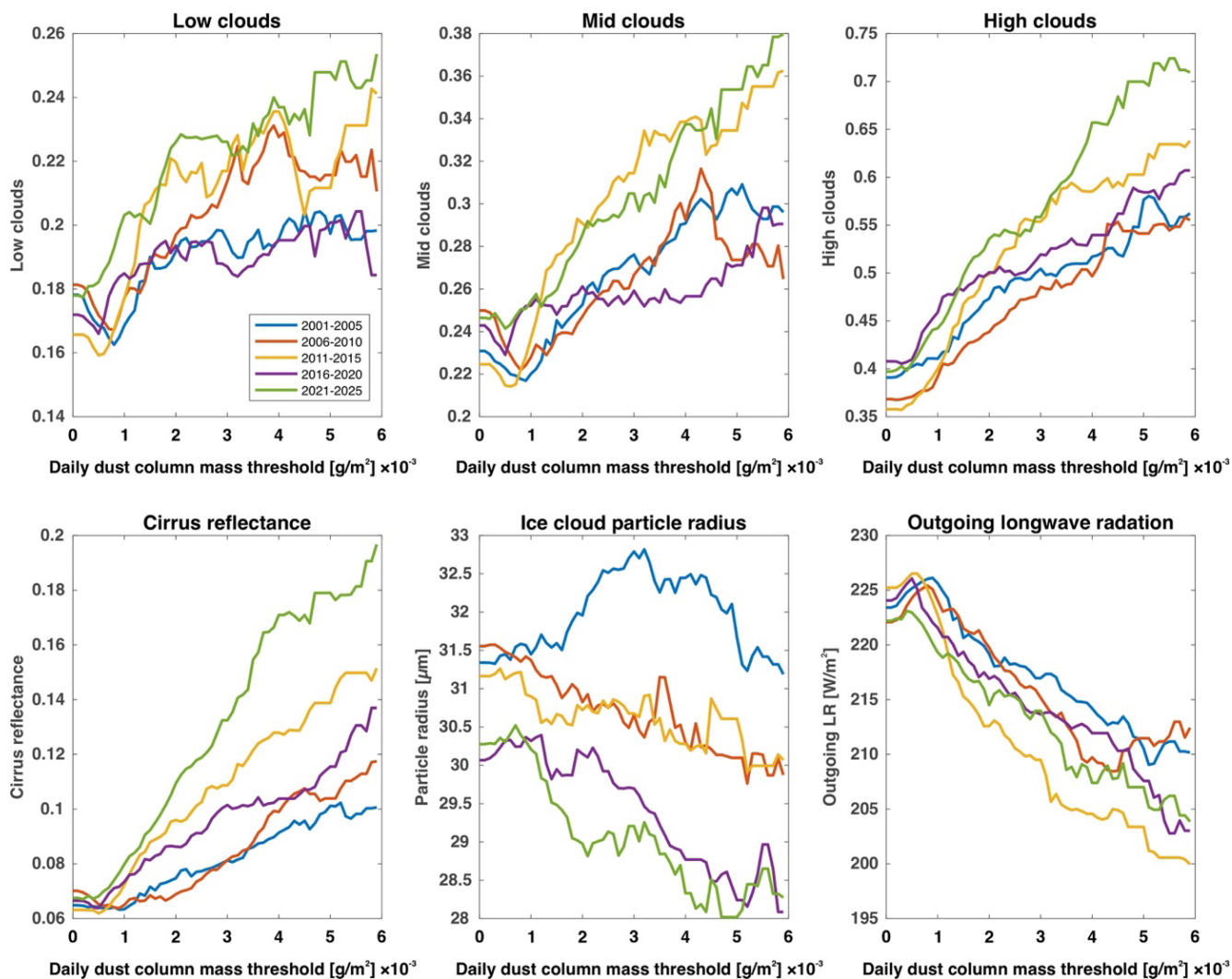
investigating dust-related heterogeneous ice nucleation processes, as well as the development and radiative impacts of upper-level ice clouds over the Carpathian Basin.

320 The springtime results reveal a clear relationship between increasing atmospheric dust loading and changes in upper-tropospheric cloud properties (Figure 2). Comparison of the five-year periods suggests that dust-associated high-level cloud formation processes have gradually intensified during the last two decades, particularly in spring.

Middle- and high-level cloud cover fractions also show a positive relationship with dust loading, whereas neither a clear trend nor a robust relationship can be identified for low cloud cover. Both the mid cloud fraction and, especially, the high cloud fraction increase with rising dust column mass density in nearly all periods, and the magnitude of this increase becomes progressively stronger over time. During 2021–2025, high cloud fraction values associated with the highest dust loads were already approximately 1.5 times greater than those observed during 2001–2005. Both cloud top pressure and cloud top temperature exhibit a pronounced decrease with increasing dust loading. Higher dust column mass density values are consistently associated with lower cloud-top pressures and colder cloud-top temperatures, particularly during the 2011–2015 and 2021–2025 periods. This indicates that dust events are increasingly linked to colder, ice-phase-dominated cloud systems developing at higher tropospheric levels.

The clearest signatures of dust–cirrus interactions emerge from changes in cirrus reflectance and ice particle size. In spring, cirrus reflectance increases with dust loading during every study period; however, the strength of this increase becomes substantially greater in the more recent intervals. Particularly pronounced reflectance enhancements are observed during 2016–2020 and 2021–2025 under elevated dust-loading conditions. Simultaneously, and in accordance with expectations, effective particle radius exhibits a gradual decrease. Smaller effective ice crystal sizes may indicate increasing ice crystal number concentrations and enhanced heterogeneous ice nucleation, consistent with the increasingly important role of Saharan mineral dust as an ice-nucleating particle.

340 These results suggest that increasing atmospheric dust loading is associated not only with a higher occurrence of upper-level cloud cover but also with significant modifications of cirrus cloud microphysical properties. The comparison of consecutive five-year periods indicates a progressive strengthening of the relationship between Saharan dust and upper-level ice clouds, particularly during the spring season.



345 **Figure 2.** Variations of the investigated atmospheric and cloud-physical parameters as a function of daily dust column mass density thresholds during the 2001–2025 period, presented in consecutive five-year time windows. (Low, middle and high level cloud coverage values are expressed as area-averaged of cloud area fraction.)

3.5. Radiative effects of dust-associated clouds

To investigate the radiative impacts of dust-associated high-level clouds, HIRS OLR data were analysed for the spring season. The results reveal again a clear relationship between increasing atmospheric dust loading and decreasing OLR values across all investigated five-year periods. As dust column mass density increases, the amount of longwave radiation emitted from the study region to space gradually decreases, a pattern that becomes particularly pronounced during the 2011–2015, 2016–2020, and 2021–2025 periods.

350



Under the highest dust-loading conditions, OLR values were approximately 15–25 W m⁻² lower than those observed during low-dust situations. (These findings are consistent with the changes observed in cloud top pressure and cloud top temperature, which indicate that dust events are increasingly associated with higher-altitude and colder ice-cloud systems.) The simultaneous increase in high cloud fraction and cirrus reflectance further suggests that dust-rich conditions favour the development of more extensive and optically thicker upper-level cloud cover.

From a radiative perspective, the observed decrease in OLR indicates that high, cold cirrus clouds retain a larger fraction of outgoing longwave radiation, thereby reducing the effective radiative emission of the surface–atmosphere system. Comparison of the consecutive five-year periods reveals a gradual strengthening of the relationship between atmospheric dust loading and OLR, particularly during the two most recent periods. This finding suggests that the radiative influence of Saharan dust-associated upper-level ice clouds has become increasingly important over the Carpathian Basin during the past two decades. The OLR anomalies associated with cirrus clouds are fully consistent with the trends identified in the cloud-physical parameters and provide additional evidence that increasing atmospheric dust loading is linked not only to changes in the frequency and optical properties of high-level cloud cover, but also to their regional radiative consequences.

4. Discussion

4.1. Evidence for strengthening dust–cloud interactions

The generalized additive model (GAM) analysis provides independent statistical support for the central finding of this study: the relationship between atmospheric dust loading and cloud properties has not remained stationary during the last 25 years. While the descriptive analyses presented in the previous sections already suggested progressively stronger associations between Saharan dust intrusions and upper-level cloud formation, the GAM framework allows these relationships to be quantified while accounting for non-linear responses and long-term temporal changes.

A particularly important result is that atmospheric dust loading emerged as a highly significant predictor of all investigated cloud and radiative variables. The consistently high adjusted R² values indicate that dust loading explains a substantial fraction of the observed variability in cloud fraction, cirrus reflectance, effective ice particle radius, and outgoing longwave radiation. This finding reinforces the interpretation that Saharan dust is closely linked to cloud formation processes throughout the troposphere.

However, the most notable outcome of the GAM analysis is the significance of the dust–time interaction term in all investigated models. Statistically, this indicates that the relationship between dust loading and cloud properties has changed over time. In other words, the cloud response associated with a given level of atmospheric dust loading differs between the early 2000s and the most recent years of the study period. This result is consistent with the patterns identified in the five-year composite analyses, where increasingly pronounced cloud responses were observed under comparable dust-loading conditions.

The strongest effects were detected for cirrus reflectance, high cloud fraction, and outgoing longwave radiation, particularly during spring. These variables also represent the most direct indicators of upper-tropospheric ice-cloud development and their



385 radiative consequences. The agreement between the GAM results and the independently derived cloud-physical indicators strengthens confidence that the observed changes do not simply reflect random variability or isolated extreme events. Instead, they point toward a systematic modification of the dust–cloud relationship over time.

The significant responses identified for effective ice particle radius are particularly noteworthy. Smaller effective radii associated with increasing dust loading are consistent with the expected microphysical response to enhanced concentrations of ice-nucleating particles. Although the GAM analysis itself does not provide direct evidence of heterogeneous ice nucleation, 390 the statistical signal is fully compatible with the physical interpretation derived from the observed changes in cirrus reflectance and cloud fraction.

Equally important is the finding that significant dust-related responses were detected not only for high-level clouds but also for middle-level cloud cover. This suggests that the influence of Saharan dust may extend beyond classical cirrus formation and potentially affect cloud systems developing within the mixed-phase temperature regime. The presence of significant dust– 395 time interactions in middle-cloud fraction indicates that the strengthening aerosol–cloud relationships identified in this study may involve multiple cloud types and atmospheric layers.

Taken together, the GAM results support the conclusion that the observed changes cannot be explained solely by an increase in the frequency of Saharan dust intrusions. If dust frequency alone were responsible, one would expect increasing numbers 400 of dusty events but relatively stable dust–cloud relationships. Instead, the statistically significant interaction between dust loading and time suggests that the atmospheric response to dust has itself evolved during the study period. This finding is consistent with the hypothesis that long-term changes in upper-tropospheric thermodynamic conditions have increasingly favoured cloud formation during dust intrusions.

Consequently, the GAM analysis provides quantitative evidence that the influence of Saharan dust on cloud formation 405 processes over the Carpathian Basin has strengthened during the last two and a half decades. While the underlying physical mechanisms require further investigation, the statistical results clearly demonstrate that dust-associated cloud responses have become progressively more pronounced across multiple cloud and radiative indicators.

The results of this study clearly indicate that the relationship between Saharan dust and upper-level ice clouds over the Carpathian Basin has strengthened progressively during the past 25 years. Increasing atmospheric dust loading was associated 410 with greater high cloud cover, enhanced cirrus reflectance, smaller effective ice crystal radii, and reduced outgoing longwave radiation. These findings suggest that the role of mineral dust extends beyond its direct aerosol effects and increasingly influences cloud formation and radiative processes in the upper troposphere.

4.2. Connection to increase of ice-supersaturated regions

Our results are consistent with recent studies reporting an increasing frequency of high relative humidity and ice-supersaturated 415 conditions across the mid-latitudes of the Northern Hemisphere. Recent investigations suggest that the most pronounced change is not necessarily an increase in mean upper-tropospheric humidity, but rather a growing frequency of humidity conditions that are critical for cirrus formation (Benetatos et al., 2024). Because ice-supersaturated regions represent the



primary thermodynamic environment for natural cirrus development, their increasing occurrence may provide increasingly favourable conditions for heterogeneous ice nucleation. Under such conditions, the long-term increase in Saharan dust transport may act as an efficient source of ice-nucleating particles, contributing to more frequent formation of dust-associated cirrus clouds and an increasing radiative influence of these clouds over Central Europe (Varga et al., 2026; Weger et al., 2018). The observed strengthening of dust-related cirrus formation cannot be explained solely by changes in aerosol availability. It is likely also linked to ongoing modifications in the thermodynamic structure of the upper troposphere. Our previous studies have shown that the increasing frequency of Saharan dust intrusions reaching the Carpathian Basin may be related to the increasingly meridional and meandering character of the jet stream, which enhances the northward transport of dust-laden air masses from the Mediterranean and North Africa (Varga, 2020). The jet-stream environment is simultaneously recognized as one of the most important regions for ISSR formation, as frontal zones, upper-tropospheric divergence, and large-scale ascent associated with jet dynamics promote the development of ice-saturated and ice-supersaturated conditions (Hildebrandt et al., 2026; Spichtinger et al., 2005). Consequently, the jet stream and the mid-latitude storm tracks jointly regulate both upper-tropospheric moisture conditions and the thermodynamic prerequisites for cirrus formation. Eleftheratos et al. (2007) likewise demonstrated that cirrus cloud variability is closely linked to upper-tropospheric humidity and vertical motions, and that European cirrus variability is partly controlled by the North Atlantic Oscillation and associated circulation patterns. Our results therefore suggest that the increasing frequency of meridional circulation patterns may exert a dual influence over Central Europe by simultaneously enhancing Saharan dust transport and increasing the occurrence of ISSRs favourable for heterogeneous ice nucleation.

Recent studies investigating upper-tropospheric humidity (UTH) conditions suggest that the average moisture content of the upper troposphere does not necessarily exhibit a strong long-term increase (globally, ice-relative UTH has increased by approximately +0.15% per decade). Instead, the frequency of high relative humidity conditions with respect to ice, including saturated and supersaturated states, has increased more substantially, by approximately +0.3 to +0.7% per decade (Benetatos et al., 2024). This strengthening of the upper tail of the humidity distribution is particularly important for cirrus cloud formation, as these relatively short-lived but microphysically critical conditions promote ice nucleation and support the persistence of extensive cirrus cloud layers. So, primarily the frequency of ice-saturated and ice-supersaturated conditions, rather than mean upper-tropospheric humidity itself, that has increased during recent decades. Although climate models do not show a completely consistent signal regarding future ISSR occurrence over the Northern Hemisphere mid-latitudes (40–60°N), several studies suggest a modest increase. Benetatos et al. (2024) demonstrated that between 1979 and 2020 both upper-tropospheric humidity and the occurrence frequency of ice-saturated and supersaturated conditions increased over the mid-latitudes, with the latter exhibiting an even stronger trend. Particularly noteworthy is the finding that occurrences of high UTHi values (>70%, >80%, >90%, and >100%) increased significantly throughout the 30–60°N latitude belt, implying that environmental conditions favourable for cirrus formation have become progressively more common.



450 Regional European studies provide additional support for the mechanisms proposed here. Lidar observations from southern France (Hoareau et al., 2013) and Rome (Gobbi et al., 2004) demonstrate that cirrus clouds are frequent and climatologically important features of the European mid-latitude atmosphere. Cirrus occurrence frequencies of approximately 37–54% were reported over southern France, while cirrus clouds were observed on nearly 45% of measurement days over Rome. In both regions, maximum frequencies occurred during the spring and autumn transition seasons.

455 The Italian observations are particularly relevant in the context of aerosol–cirrus interactions. Over Rome, Saharan dust was present on approximately 20% of observation days, primarily within the 2–6 km altitude range between boundary-layer aerosols and cirrus layers located between 6 and 14 km. Dust-influenced situations frequently exhibited larger cirrus optical thickness and enhanced backscatter compared with dust-free conditions, suggesting that Saharan mineral particles may efficiently promote cirrus formation through heterogeneous ice nucleation. Together, these studies indicate that cirrus cloud
460 properties across the Mediterranean and southern Europe are influenced not only by meteorological conditions but also by long-range transported aerosols, particularly Saharan mineral dust, which regularly reaches the region and may provide effective ice-nucleating particles for upper-tropospheric cloud formation.

Direct observational evidence for this mechanism was provided by (Ansmann et al., 2019b) using combined lidar and radar measurements over Cyprus. The authors found a close correspondence between predicted INP concentrations and observed
465 ice crystal concentrations within Saharan dust-containing middle- and upper-tropospheric cloud layers. The investigated cirrus clouds formed at altitudes between 8 and 11 km and temperatures ranging from -35 to -57 °C, and in several cases the observed ice crystal concentrations could be fully explained by the available dust-derived INPs. Particularly noteworthy is the “dust-infused baroclinic storm” (DIBS) case described by the authors, in which a North African dust outbreak injected large quantities of Saharan dust into the upper troposphere. The resulting dust-enriched cirrus system could be tracked for more than
470 3,500 km from the Mediterranean to Central Asia, and the study concluded that mineral dust substantially contributed to the persistence and longevity of the cirrus cloud system. Similar dust-cirrus interactions were described in detail by other (Central) European studies (Seifert et al., 2023; Weger et al., 2018). This mechanism provides a plausible physical explanation for the patterns identified in the present study, whereby increasing dust loading is associated with greater high cloud cover, enhanced cirrus reflectance, and smaller effective ice crystal sizes over the Carpathian Basin.

475 **4.3. Possible implications for mixed-phase cloud formation**

Although the present study primarily focuses on cirrus clouds, the observed increase in mid-level cloud fraction with increasing atmospheric dust loading suggests that Saharan mineral dust may also influence cloud processes outside the classical cirrus regime. Mixed-phase clouds, containing both supercooled liquid droplets and ice crystals, frequently occur within the temperature range between approximately 0 and -38 °C and represent one of the largest remaining uncertainties in aerosol–
480 cloud interactions and climate feedbacks (Storelvmo, 2017).



Mineral dust particles are known to be highly efficient ice-nucleating particles not only under cirrus-forming conditions but also within mixed-phase clouds (Atkinson et al., 2013; Hoose et al., 2008; Wiacek et al., 2010). Enhanced concentrations of dust-derived INPs may promote heterogeneous freezing of supercooled droplets, thereby accelerating glaciation processes and modifying cloud lifetime, cloud fraction, precipitation formation, and radiative properties. Depending on thermodynamic conditions, increased ice formation may either enhance precipitation and cloud dissipation through the Wegener–Bergeron–Findeisen process or increase cloud persistence through continuous ice crystal production.

The positive relationship observed between atmospheric dust loading and middle-level cloud fraction in the present study is therefore noteworthy. Although the available datasets do not allow direct identification of mixed-phase cloud processes, the observed behaviour is consistent with the possibility that Saharan dust influences not only upper-tropospheric cirrus clouds but also cloud systems developing within the mixed-phase temperature regime. If confirmed by future investigations using vertically resolved cloud observations and thermodynamic profiles, this mechanism would imply that the climatic influence of Saharan dust over Central Europe extends beyond cirrus cloud formation and may affect a broader spectrum of cloud types and associated radiative processes.

4.4. Radiative implications

The radiative implications identified in this study are consistent with recent findings reported in the international literature. Cirrus clouds occupy a unique position within the Earth's radiation budget because, unlike most cloud types, they exhibit a relatively limited ability to reflect incoming shortwave radiation while efficiently absorbing and re-emitting outgoing longwave radiation from the surface and lower troposphere. As a result, optically thin and moderately thick cirrus clouds generally exert a net warming effect, primarily manifested through a reduction in outgoing longwave radiation.

In a twenty-year lidar-based study conducted over Greenbelt, Maryland, Lolli et al. (2026) demonstrated that the radiative effects of cirrus clouds exhibit measurable long-term trends and that changes in cloud–radiation interactions play an important role in regional energy budgets. The authors emphasized that long-term monitoring of the optical and microphysical properties of cirrus clouds is essential for understanding radiative processes associated with climate change.

Our findings can also be placed within a broader climatological context provided by recent satellite-based radiation studies. Studies showed that the radiative characteristics of the Northern Hemisphere have undergone substantial changes during the past two decades, driven by combined variations in aerosols, atmospheric moisture, and cloud cover (Hodnebrog et al., 2024; Loeb et al., 2021). According to their results, cloud–radiation interactions represent one of the key contributors to the development of hemispheric radiative asymmetries. The increasing cirrus cloud cover, enhanced cirrus reflectance, and decreasing OLR observed over the Carpathian Basin may therefore be interpreted as a regional manifestation of these larger-scale processes. Our results suggest that Saharan mineral dust at mid-latitudes may influence not only the microphysical properties of clouds but also contribute to changes in upper-tropospheric energy exchange through the increasing radiative significance of high-level ice clouds.



5. Conclusions

The aim of this study was to investigate the relationship between Saharan mineral dust and upper-level ice clouds over the
515 Carpathian Basin during the period 2001–2025. Using independent satellite and reanalysis datasets (MERRA-2, MODIS, and
HIRS), we found a progressively strengthening association between atmospheric dust loading and cirrus cloud properties.
Mean dust column mass increased by nearly 55%, from 0.0059 to 0.0091 g m⁻², between the weakest and strongest cirrus-
affected events, while the mean effective ice particle radius decreased from 30.3 to 28.2 μm. During the study period, the
number of dust events with high-cloud fractions above the upper quartile increased from 8 to 19–20, and those with cirrus
520 reflectance above the upper quartile from 11 to 19. These relationships were strongest in spring, which accounted for 116 of
the 276 Saharan dust events (42%) and exhibited the highest mean dust loading (0.008 g m⁻²). Spring also yielded the strongest
GAM performance (adjusted R² = 0.996 for cirrus reflectance and 0.993 for high-cloud fraction).

The strengthening dust–cloud relationship was further supported by progressively lower outgoing longwave radiation (OLR)
under dusty conditions. During spring, OLR decreased by approximately 15–25 W m⁻² between low- and high-dust situations,
525 while the GAM analysis showed an excellent model fit (adjusted R² = 0.988) and a highly significant dust–time interaction,
indicating that dust-associated cirrus clouds have become increasingly extensive and/or optically thicker over time. Together,
these results show that the climatic influence of Saharan dust over Central Europe extends beyond its direct radiative effects
and increasingly involves cloud-mediated processes.

Our findings are consistent with previous studies identifying Saharan dust as an efficient source of ice-nucleating particles and
530 with recent evidence for increasing ice-supersaturated conditions in the mid-latitude upper troposphere. However, this study
advances current knowledge by demonstrating that the strength of the dust–cirrus relationship itself has increased over the past
25 years. This suggests that changes in the upper-tropospheric thermodynamic environment have enhanced the efficiency of
mineral dust in promoting cirrus formation.

The study is based on satellite observations and reanalysis products and therefore infers physical mechanisms from robust
535 statistical relationships rather than direct in situ observations. Although the agreement among multiple independent datasets
increases confidence in the results, the relative contributions of dust mineralogy, transport pathways, upper-tropospheric
humidity, and atmospheric circulation remain unresolved and should be addressed by future observational and modelling
studies.

Saharan dust has become an increasingly important regulator of upper-level cloud formation and radiative processes over
540 Central Europe. The observed strengthening of dust–cirrus interactions implies that future changes in atmospheric circulation
and upper-tropospheric moisture may amplify the climatic influence of mineral dust through aerosol–cloud interactions. Better
representation of these evolving processes in weather and climate models will therefore be essential for improving estimates
of regional cloud feedbacks and radiative forcing.



545 Acknowledgments

The research was supported by the NRD1 projects FK138692. This work has been implemented by the National Multidisciplinary Laboratory for Climate Change (RRF-2.3.1-21-2022-00014) project within the framework of Hungary's National Recovery and Resilience Plan supported by the Recovery and Resilience Facility of the European Union. The research was funded by the Sustainable Development and Technologies National Programme of the Hungarian Academy of Sciences (FFT NP FTA). This work was supported by the Ministry for Innovation and Technology of Hungary from the National Research, Development and Innovation Fund, financed under the 2021 Thematic Excellence Program funding scheme (grant number TKP2021-NKTA-21).

Data availability

Data will be made available on request.

555 Author contributions

Conceptualization: GV, AG, ÁR

Methodology: GV, FG, AC

Investigation: GV

Visualization: FG, AC, ÁR

560 Writing—original draft: GV

Writing—review & editing: AG, ÁR

Competing interests

Authors declare that they have no competing interests

References

- 565 Andreae, M. O. and Rosenfeld, D.: Aerosol–cloud–precipitation interactions. Part 1. The nature and sources of cloud-active aerosols, *Earth. Sci. Rev.*, 89, 13–41, <https://doi.org/10.1016/j.earscirev.2008.03.001>, 2008.
- Ansmann, A., Mamouri, R., Bühl, J., Seifert, P., Engelmann, R., Hofer, J., Nisantzi, A., Atkinson, J., Kanji, Z., Sierau, B., Vrekoussis, M., and Sciare, J.: Ice-nucleating particle versus ice crystal number concentration in altocumulus and cirrus layers embedded in Saharan dust: a closure study, *Atmos. Chem. Phys.*, 19, 15087–15115, [https://doi.org/10.5194/ACP-19-15087-](https://doi.org/10.5194/ACP-19-15087-2019)
- 570 2019, 2019a.



- Ansmann, A., Mamouri, R., Bühl, J., Seifert, P., Engelmann, R., Nisantzi, A., Hofer, J., and Baars, H.: Lidar/radar approach to quantify the dust impact on ice nucleation in mid and high level clouds, *E3S Web of Conferences*, <https://doi.org/10.1051/E3SCONF/20199904003>, 2019b.
- Atkinson, J. D., Murray, B. J., Woodhouse, M. T., Whale, T. F., Baustian, K. J., Carslaw, K. S., Dobbie, S., O'Sullivan, D.,
575 and Malkin, T. L.: The importance of feldspar for ice nucleation by mineral dust in mixed-phase clouds, *Nature*, 498, 355–358, <https://doi.org/10.1038/nature12278>, 2013.
- Benetatos, C., Eleftheratos, K., Gierens, K., and Zerefos, C.: A statistically significant increase in ice supersaturation in the atmosphere in the past 40 years, *Sci. Rep.*, 14, 24760, <https://doi.org/10.1038/s41598-024-75756-9>, 2024.
- Boucher, O., Randall, D., Artaxo, P., Bretherton, C., Feingold, G., Forster, P., Kerminen, V.-M., Kondo, Y., Liao, H., and
580 Lohmann, U.: Clouds and aerosols, in: *Climate change 2013: The physical science basis. Contribution of working group I to the fifth assessment report of the intergovernmental panel on climate change*, Cambridge University Press, 571–657, 2013.
- Chatziparaschos, M., Daskalakis, N., Myriokefalitakis, S., Kalivitis, N., Nenes, A., Gonçalves Ageitos, M., Costa-Surós, M., Pérez García-Pando, C., Zanolli, M., Vrekoussis, M., and Kanakidou, M.: Role of K-feldspar and quartz in global ice nucleation by mineral dust in mixed-phase clouds, *Atmos. Chem. Phys.*, 23, 1785–1801, <https://doi.org/10.5194/acp-23-1785-2023>, 2023.
- 585 Cuevas-Agulló, E., Barriopedro, D., García, R., Alonso-Pérez, S., González-Alemán, J. J., Werner, E., Suárez, D., Bustos, J. J., García-Castrillo, G., García, O., Barreto, Á., and Basart, S.: Sharp increase in Saharan dust intrusions over the western Euro-Mediterranean in February–March 2020–2022 and associated atmospheric circulation, *Atmos. Chem. Phys.*, <https://doi.org/10.5194/acp-24-4083-2024>, 2024.
- Eleftheratos, K., Zerefos, C. S., Zanis, P., Balis, D. S., Tselioudis, G., Gierens, K., and Sausen, R.: A study on natural and
590 manmade global interannual fluctuations of cirrus cloud cover for the period 1984–2004, *Atmos. Chem. Phys.*, 7, 2631–2642, <https://doi.org/10.5194/acp-7-2631-2007>, 2007.
- Gobbi, G. P., Barnaba, F., and Ammannato, L.: The vertical distribution of aerosols, Saharan dust and cirrus clouds in Rome (Italy) in the year 2001, *Atmos. Chem. Phys.*, 4, 351–359, <https://doi.org/10.5194/acp-4-351-2004>, 2004.
- Harrison, A. D., Lever, K., Sanchez-Marroquin, A., Holden, M. A., Whale, T. F., Tarn, M. D., McQuaid, J. B., and Murray,
595 B. J.: The ice-nucleating ability of quartz immersed in water and its atmospheric importance compared to K-feldspar, *Atmos. Chem. Phys.*, 19, 11343–11361, <https://doi.org/10.5194/acp-19-11343-2019>, 2019.
- Hildebrandt, K. G., Castino, F., Meijer, V., and Yin, F.: Variability of ice supersaturated regions at flight altitudes: evaluation of ERA5 reanalysis using IAGOS in situ measurements, *Atmos. Chem. Phys.*, 26, 6449–6470, <https://doi.org/10.5194/acp-26-6449-2026>, 2026.
- 600 Hoareau, C., Keckhut, P., Noel, V., Chepfer, H., and Baray, J.-L.: A decadal cirrus clouds climatology from ground-based and spaceborne lidars above the south of France (43.9° N–5.7° E), *Atmos. Chem. Phys.*, 13, 6951–6963, <https://doi.org/10.5194/acp-13-6951-2013>, 2013.



- Hodnebrog, Ø., Myhre, G., Jouan, C., Andrews, T., Forster, P. M., Jia, H., Loeb, N. G., Olivié, D. J. L., Paynter, D., Quaas, J., Raghuraman, S. P., and Schulz, M.: Recent reductions in aerosol emissions have increased Earth's energy imbalance, *Commun. Earth Environ.*, 5, 166, <https://doi.org/10.1038/s43247-024-01324-8>, 2024.
- 605 Hoose, C. and Möhler, O.: Heterogeneous ice nucleation on atmospheric aerosols: a review of results from laboratory experiments, *Atmos. Chem. Phys.*, 12, 9817–9854, <https://doi.org/10.5194/acp-12-9817-2012>, 2012.
- Hoose, C., Lohmann, U., Erdin, R., and Tegen, I.: The global influence of dust mineralogical composition on heterogeneous ice nucleation in mixed-phase clouds, *Environmental Research Letters*, 3, 025003, <https://doi.org/10.1088/1748-9326/3/2/025003>, 2008.
- 610 Irvine, E. A. and Shine, K. P.: Ice supersaturation and the potential for contrail formation in a changing climate, *Earth System Dynamics*, 6, 555–568, <https://doi.org/10.5194/esd-6-555-2015>, 2015.
- Kärcher, B.: Formation and radiative forcing of contrail cirrus, *Nat. Commun.*, 9, 1824, <https://doi.org/10.1038/s41467-018-04068-0>, 2018.
- 615 Kok, J. F., Storelvmo, T., Karydis, V. A., Adebisi, A. A., Mahowald, N. M., Evan, A. T., He, C., and Leung, D. M.: Mineral dust aerosol impacts on global climate and climate change, *Nat. Rev. Earth Environ.*, 4, 71–86, <https://doi.org/10.1038/s43017-022-00379-5>, 2023.
- Loeb, N. G., Johnson, G. C., Thorsen, T. J., Lyman, J. M., Rose, F. G., and Kato, S.: Satellite and Ocean Data Reveal Marked Increase in Earth's Heating Rate, *Geophys. Res. Lett.*, 48, e2021GL093047, <https://doi.org/10.1029/2021GL093047>, 2021.
- 620 Lolli, S., Dolinar, E. K., Lewis, J. R., Salcedo-Bosch, A., Campbell, J. R., and Welton, E. J.: Long-term trends in daytime cirrus cloud radiative effects: analyzing twenty years of Micropulse Lidar Network measurements at Greenbelt, Maryland in eastern North America, *Atmos. Chem. Phys.*, 26, 411–426, <https://doi.org/10.5194/acp-26-411-2026>, 2026.
- Pey, J., Querol, X., Alastuey, A., Forastiere, F., and Stafoggia, M.: African dust outbreaks over the Mediterranean Basin during 2001–2011: PM₁₀ concentrations, phenomenology and trends, and its relation with synoptic and mesoscale meteorology, *Atmos. Chem. Phys.*, 13, 1395–1410, <https://doi.org/10.5194/acp-13-1395-2013>, 2013.
- 625 Rodríguez, S. and López-Darias, J.: Extreme Saharan dust events expand northward over the Atlantic and Europe, prompting record-breaking PM₁₀ and PM_{2.5} episodes, *Atmos. Chem. Phys.*, 24, 12031–12053, <https://doi.org/10.5194/acp-24-12031-2024>, 2024.
- 630 Rogora, M., Mosello, R., and Marchetto, A.: Long-term trends in the chemistry of atmospheric deposition in Northwestern Italy: the role of increasing Saharan dust deposition, *Tellus B: Chemical and Physical Meteorology*, 56, 426–434, <https://doi.org/10.3402/tellusb.v56i5.16456>, 2004.
- Salvador, P., Pey, J., Pérez, N., Querol, X., and Artíñano, B.: Increasing atmospheric dust transport towards the western Mediterranean over 1948–2020, *NPJ Clim. Atmos. Sci.*, 5, <https://doi.org/10.1038/s41612-022-00256-4>, 2022.



- 635 Sassen, K. and Campbell, J. R.: A Midlatitude Cirrus Cloud Climatology from the Facility for Atmospheric Remote Sensing. Part I: Macrophysical and Synoptic Properties, *J. Atmos. Sci.*, 58, 481–496, [https://doi.org/10.1175/1520-0469\(2001\)058<0481:AMCCCF>2.0.CO;2](https://doi.org/10.1175/1520-0469(2001)058<0481:AMCCCF>2.0.CO;2), 2001.
- Seifert, A., Bachmann, V., Filipitsch, F., Förstner, J., Grams, C., Hoshyaripour, G., Quinting, J., Rohde, A., Vogel, H., Wagner, A., and Vogel, B.: Aerosol–cloud–radiation interaction during Saharan dust episodes: the dusty cirrus puzzle, *Atmos. Chem. Phys.*, <https://doi.org/10.5194/acp-23-6409-2023>, 2023.
- 640 Seifert, P., Ansmann, A., Mattis, I., Wandinger, U., Tesche, M., Engelmann, R., Müller, D., García-Pando, C. P., and Hausteiner, K.: Saharan dust and heterogeneous ice formation: Eleven years of cloud observations at a central European EARLINET site, *J. Geophys. Res.*, 115, <https://doi.org/10.1029/2009JD013222>, 2010.
- Spichtinger, P., Gierens, K., and Dörnbrack, A.: Formation of ice supersaturation by mesoscale gravity waves, *Atmos. Chem. Phys.*, 5, 1243–1255, <https://doi.org/10.5194/acp-5-1243-2005>, 2005.
- 645 Stein, A. F., Draxler, R. R., Rolph, G. D., Stunder, B. J. B., Cohen, M. D., and Ngan, F.: NOAA’s hysplit atmospheric transport and dispersion modeling system, <https://doi.org/10.1175/BAMS-D-14-00110.1>, 1 December 2015.
- Storelvmo, T.: Aerosol Effects on Climate via Mixed-Phase and Ice Clouds, *Annu. Rev. Earth Planet. Sci.*, 45, 199–222, <https://doi.org/10.1146/annurev-earth-060115-012240>, 2017.
- 650 Twomey, S.: Pollution and the planetary albedo, *Atmospheric Environment* (1967), 8, 1251–1256, [https://doi.org/10.1016/0004-6981\(74\)90004-3](https://doi.org/10.1016/0004-6981(74)90004-3), 1974.
- Varga, G.: Changing nature of Saharan dust deposition in the Carpathian Basin (Central Europe): 40 years of identified North African dust events (1979–2018), *Environ. Int.*, 139, <https://doi.org/10.1016/j.envint.2020.105712>, 2020.
- Varga, G., Kovács, J., and Újvári, G.: Analysis of Saharan dust intrusions into the Carpathian Basin (Central Europe) over the period of 1979–2011, *Glob. Planet. Change*, 100, <https://doi.org/10.1016/j.gloplacha.2012.11.007>, 2013.
- 655 Varga, G., Gresina, F., Gelencsér, A., Csávic, A., and Rostási, Á.: Saharan dust and cirrus clouds: Dominating indirect impact of dust events on photovoltaic energy generation in Hungary (2019–2024), *Solar Energy*, 307, 114385, <https://doi.org/10.1016/j.solener.2026.114385>, 2026.
- Weger, M., Heinold, B., Engler, C., Schumann, U., Seifert, A., Föbög, R., Voigt, C., Baars, H., Blahak, U., Borrmann, S., Hoose, C., Kaufmann, S., Krämer, M., Seifert, P., Senf, F., Schneider, J., and Tegen, I.: The impact of mineral dust on cloud formation during the Saharan dust event in April 2014 over Europe, *Atmos. Chem. Phys.*, 18, 17545–17572, <https://doi.org/10.5194/acp-18-17545-2018>, 2018.
- 660 Wiacek, A., Peter, T., and Lohmann, U.: The potential influence of Asian and African mineral dust on ice, mixed-phase and liquid water clouds, *Atmos. Chem. Phys.*, 10, 8649–8667, <https://doi.org/10.5194/ACP-10-8649-2010>, 2010.